Evidence of a Symmetry-Dependent Metallic Barrier in Fully Epitaxial MgO Based Magnetic Tunnel Junctions

F. Greullet,[1] C. Tiusan,[1] F. Montaigne,[1] M. Hehn,[1] D. Halley,[2] O. Bengone,[2] M. Bowen,[2] and W. Weber[2]
[1]*LPM, UMR CNRS 7556, Nancy Université, Boulevard des Aiguillettes, BP 239, 54506 Vandœuvre-lès-Nancy Cedex, France*
[2]*IPCMS, UMR CNRS 7504, Université Louis Pasteur, 23 rue de Loess, BP 43, 67034, Strasbourg Cedex 2, France*
(Received 30 January 2007; revised manuscript received 9 August 2007; published 1 November 2007)

We report on the experimental observation of tunneling across an ultrathin metallic Cr spacer layer that is inserted at the interface of a Fe/MgO/Fe(001) junction. We show how this remarkable behavior in a solid-state device reflects a quenching in the transmission of particular electronic states, as expected from the symmetry-filtering properties of the MgO barrier and the band structure of the bcc Cr(001) spacer in the epitaxial junction stack. This ultrathin Cr metallic barrier can promote quantum well states in an adjacent Fe layer.

DOI: 10.1103/PhysRevLett.99.187202 PACS numbers: 85.75.−d, 73.40.Gk, 73.40.Rw

The field of magnetoelectronics, as it enters new domains, is also experiencing a consolidation of its foundations. The giant magnetoresistance (GMR) effect, originally discovered on Fe/Cr multilayers [1], was described at an early stage in terms of an interplay of band structures between a magnetic metal and a nonmagnetic metal spacer layer [2]. On the other hand, an equivalent level of comprehension of the tunneling magnetoresistance (TMR) effect between a magnetic metal and an insulating spacer layer has only recently emerged, beyond the pioneering experiments on magnetic tunnel junctions (MTJs) with an amorphous Al_2O_3 barrier [3], through the study of fully epitaxial MTJs. In fact, a convergence between experiment [4–8] and theory [9,10] regarding the symmetry-filtered spin-polarized tunneling across a MgO(001) barrier is now fully apparent with values of TMR that currently reach 1000% [11]. Indeed, electrons with Δ_1 electronic symmetry tunnel across MgO(001) with respect to a barrier of lowest energy, while electrons with other symmetries perceive larger barrier heights and are thus filtered away. The integration of this barrier into an epitaxial MTJ with bcc-ordered Fe-Co alloy electrodes [12–14], which exhibit Δ_1 electrons for only one spin projection [see Fig. 1(a)], results for the antiparallel (AP) configuration of electrode magnetizations in a tunneling current of $\Delta_1^{\uparrow}$ electrons that cannot find available spin-$\downarrow$ states in the collecting electrode with that symmetry. This in turn leads to the large TMR effect.

This large spintronic response thus reflects the conservation of two properties: spin and symmetry of the tunneling electron in the junction AP state once it enters, and continues to tunnel through, the metallic counterelectrode. The conservation of both properties can be tested by inserting a suitable spacer layer at the MTJ interface. To date, this test was performed on polycrystalline MTJs, oftentimes with an amorphous Al_2O_3 barrier. An early study revealed that the spin can be conserved during the post-tunneling conduction process in a ferromagnetic spacer over 8 Å [15]. Such ferromagnetic spacers at MTJ interfaces were shown by Nagahama *et al.* to bear quantum well (QW) states [16]. Nonmagnetic metallic spacers such as Au [17], Cr [18,19], and Ru [20] were also investigated. The effect on the transport of spin-polarized QW states within a Cu spacer was observed [21]—a result that effectively launched the convergence between GMR and TMR magnetoelectronics [22].

Yet in all instances, the insertion of the spacer dramatically quenched the TMR amplitude and any spintronic effects. Notably, recent experiments revealed minute oscillations in TMR amplitude with increasing Cr spacer thickness with a 2 monolayer (ML) period corresponding to the Cr spin sublattice [19]. This was attributed to spin scattering at the Al_2O_3/Cr(001) interface, i.e., in a *diffusive*

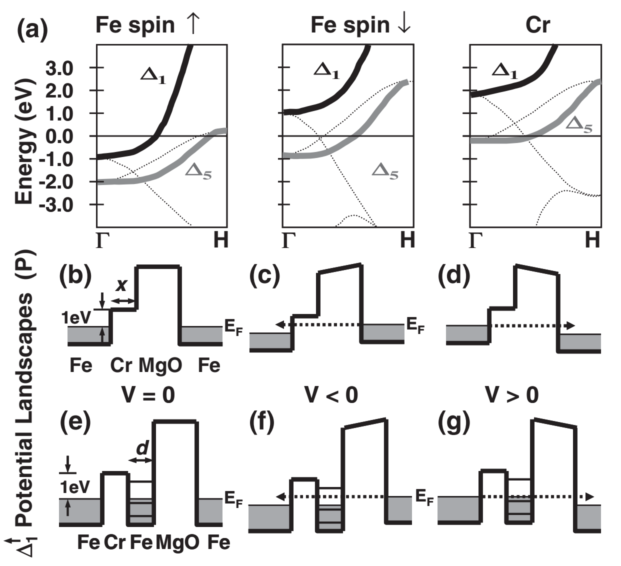

FIG. 1. (a) Band structures along the $\Gamma - H$ direction of electron propagation, of spin-polarized bcc Fe and bcc Cr, with Δ_1 (Δ_5) bands in black (gray). Panels (b)–(g): Schematics of the two MTJ potential landscapes for Δ_1 spin-$\uparrow$ electrons in the parallel (P) junction state at zero, negative, and positive bias.

transport regime that destroys the conservation of symmetry due to the amorphous structure of the Al_2O_3 barrier. Thus, the use of spacers to study the symmetry property of electron tunneling requires fully epitaxial MTJs that preserve the two-dimensional periodicity across the junction, thereby conserving the electron momentum parallel to the interface $k_{\|}$ and the coherence of the tunneling process. In this vein, some of us have experimentally demonstrated how electrons with a precise symmetry [23] tunnel with respect to symmetry-resolved states in the insulating barrier, and continue as hot electrons to tunnel despite the presence of available states if these states are mismatched in symmetry with respect to the tunneling electrons [22]. As was argued then [22,23], the ability within a heterostructure for a suitably chosen metallic layer to act as an additional tunnel barrier for electrons at the Fermi level E_F represents an important opportunity for both fundamental and applied research.

We report here on spacer experiments that demonstrate explicit control over the symmetry of the tunneling electrons. We show how the dominant majority spin Δ_1 conduction channel can be quenched in fully epitaxial Fe/Cr(x ML)/MgO/Fe(001) MTJs as the thickness x of the Cr spacer layer is increased, in agreement with our theoretical calculations. The resulting bias dependence of conductance exhibits features related to the nondominant electronic symmetries that are now apparent in the tunneling transmission. Thanks to this remarkable "insulating" behavior of the ultrathin Cr metallic spacer, we observe *large and enduring* TMR for finite x, as well as QW states in a Fe spacer layer that was inserted between the Cr and MgO Δ_1 barriers. Our work on fully epitaxial devices with GMR and TMR engineering explicitly outlines the convergence between these two branches of magnetoelectronics.

MgO//MgO(10 nm)/Fe(26 nm)/Cr(x)/MgO(3 nm)/Fe(6 nm)/Co(20 nm)/Pt(3 nm) expitaxial samples were deposited by molecular beam epitaxy under ultrahigh vacuum conditions as described elsewhere [24]. A 3 nm thick MgO barrier was chosen to filter mostly Δ_1 states at the $\bar{\Gamma}$ point [9,10,22]. The thickness x of the wedge-shaped Cr spacer varies from 0 to 6 ML. Thanks to a small lattice mismatch between bcc Fe(001) and Cr(001) (1.5%), Cr(001) and MgO(001) (2.25%), and MgO(001) and Fe(001) (3.7%), the two-dimensional layer-by-layer growth and the high crystalline quality of the epitaxial Fe, Cr, and MgO layers in the stack were achieved, as witnessed through intensity oscillations in the reflection high-energy electron diffraction pattern. Thanks to the wedge shape of the Cr layer, MTJs with the same bottom electrode, barrier, and top counterelectrode but variable Cr spacer thickness can be patterned on the same wafer.

Standard Fe/MgO/Fe(001) MTJs yield 180% TMR at $T = 300$ K and $V_{dc} = 10$ mV. This amplitude reflects the mechanism of symmetry-conserved tunneling described above, but also a non-negligible contribution from nondominant electronic symmetries. Figure 2 illustrates the experimental TMR variation ($V_{dc} = 10$ mV, $T = 300$ K) with increasing Cr thickness x normalized to that found for $x = 0$. We observe a much slower TMR decrease as compared to previous studies on Al_2O_3-based MTJs with a Cr spacer [18,19]. Indeed, 40% of the initial TMR is preserved for a 4 ML Cr spacer here, compared to the previously reported total quenching [18] and subpercent TMR [19].

We argue that, while these previous results reflect a diffusive spin-polarized tunneling regime, we are witnessing the signature of a symmetry-conserved tunneling regime here. Indeed, the insertion of the Cr spacer effectively filters away the dominant contribution of the tunneling Δ_1 states so that other symmetries now dominate the junction conductance. To confirm this explanation, we have performed first-principles calculations. The electronic structure of the system is described in terms of a surface Green function technique implemented within the framework of a tight-binding linear muffin-tin orbital approach [25]. This approach allows us to simulate on an *ab initio* level the experimental conditions for transport measurements of tunnel junctions with two semi-infinite leads. The corresponding transport properties are evaluated within a Kubo-Landauer approach, based on a transmission matrix formulation within the linear response theory [26,27]. The system studied consists of Fe/Cr(x ML)/MgO(10 ML)/Fe embedded in two semi-infinite bcc(001) Fe leads. We used the atomic structure of Ref. [28]. Given the quite low conductances at large x, we had to reduce the MgO thickness compared to experiments. The trend described with increasing x would be exacerbated for larger thicknesses due to an enhanced filtering of Δ_1 states [9].

These calculations broadly reproduce (Fig. 2) the lessened TMR decrease with x. Figure 3(a) presents the conductance G for each spin channel (P$\uparrow$, P$\downarrow$, AP$\uparrow$, and AP$\downarrow$) as a function of Cr thickness x. We see that $G_{P\uparrow}$ decreases with increasing x and reaches the low conductance of the other spin channels for $x = 6$, which remain broadly constant for all x. The large drop in $G_{P\downarrow}$ for $x = 1$

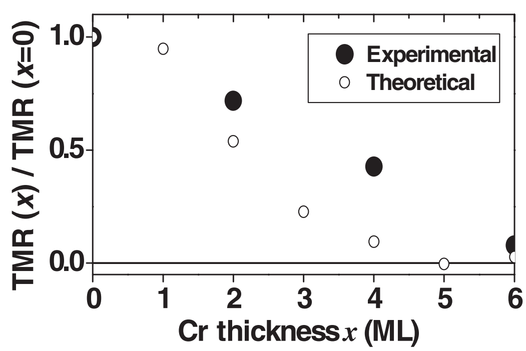

FIG. 2. Experimental and theoretical variations of normalized TMR with Cr thickness x.

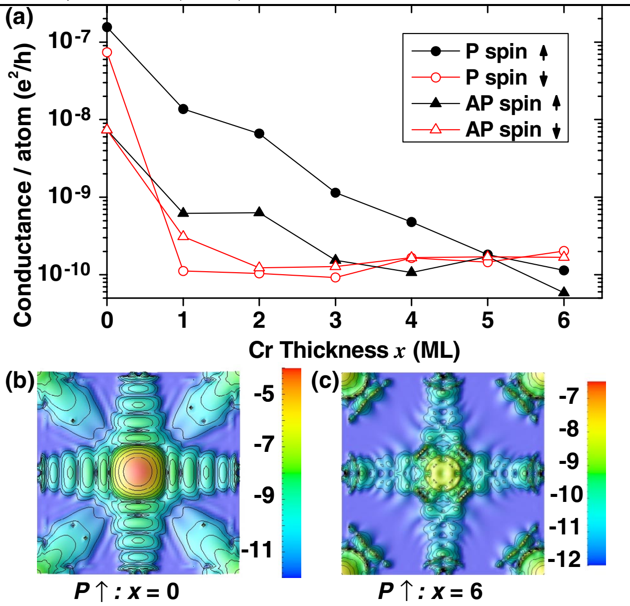

FIG. 3 (color online). Fe/Cr(x ML)/MgO(10 ML)/Fe: (a) evolution of the P↑, P↓, AP↑, and AP↓ conductance channels with increasing Cr thickness x. Transmission probability of the dominant P↑ conductance channel as a function of $k_{\|}$ for (b) $x = 0$ and (c) $x = 6$.

reflects the quenching of the Fe/MgO interface state [8]. This confirms the filtering effect of the Cr layer.

To characterize this filtering effect from a symmetry standpoint, we examine, for the dominant P↑ spin channel, the $k_{\|}$-resolved transmission probabilities for $x = 0$ [see Fig. 3(b)] and $x = 6$ [see Fig. 3(c)]. For $x = 0$, the main contribution to G arises close to the $\bar{\Gamma}$ (i.e., $k_{\|} = 0$) point, corresponding to electrons with Δ_1 symmetry [9,10]. Upon introducing the Cr spacer [Fig. 3(c) for $x = 6$], the transmission remains mainly concentrated around the $\bar{\Gamma}$ region of the two-dimensional Brillouin zone but with a strongly reduced probability. This change reflects the absence of Δ_1 states at E_F within the Cr layer [see Fig. 1(a)], which acts as an *additional* barrier for these otherwise highly transmitted Δ_1 states as schematized in Fig. 1(b). For $x = 6$, the P↑ spin channel is dominated by Δ_5 states, which have the second-smallest decay constant in MgO(001) [9,10,22] and are present at E_F both in bcc Fe(001) and bcc Cr(001).

This *controlled switch* in the symmetry of the transmitted spin-polarized carriers with the insertion of a Cr spacer experimentally results in a drop in G_P to values close to those of G_{AP}, while G_{AP} remains broadly constant. As schematized in Figs. 1(c) and 1(d), the Cr spacer acts as a barrier for Δ_1 states regardless of the direction of applied bias. At $T = 300$ K, we see a 250% increase in the resistance x area product when going from Cr thickness $x = 0$ to $x = 6$ ML for our smallest 10×10 μm^2 MTJs. It decreases to 210% for 30×30 μm^2 MTJs, which may reflect the incidence of structural defects on this effect.

Figure 4 illustrates the relative variation of G with applied bias, $\Delta G(V) = [G(V) - G(V = 0)]/G(V = 0)$ for (a) $x = 0$ and (b) $x = 6$. All these panels reveal the incidence on G of the Fe $\Delta_5^{\downarrow}$ band edge located at $E = E_F + 0.25$ eV (see arrows). Indeed, starting from $V = 0$, $\Delta G_P(V)/G_P(0)$ for $x = 0$ decreases and reaches two minima located at $|V| = 0.25$ V. For $|V| > 0.25$ V, $\Delta G_P(V)/G_P(0)$ increases strongly. Assuming a MTJ bias model of rigidly shifting the electrode Fermi levels [29] and within a multichannel model [24] of symmetry-conserved tunneling, this reflects a dominant conduction of Δ_1 electrons as well as a much smaller contribution from Δ_5 states. Once the Fe $\Delta_5^{\downarrow}$ band edge is reached, the Δ_1 contribution to conduction completely dominates and $\Delta G_P(V)/G_P(0)$ rises quickly. These signatures of Δ_1 dominant conduction in $\Delta G_P(V)/G_P(0)$ with $x = 0$ are absent for $x = 6$ [Fig. 4(b)]. Instead, $\Delta G_P(V)/G_P(0)$ exhibits the same signature as $\Delta G_{AP}(V)/G_{AP}(0)$: starting from $V = 0$, the rapid rise in conductance, before a lessened increase past $V = 0.25$ V, reflects the quenching of one of the Δ_5 conduction channels as the Fe $\Delta_5^{\downarrow}$ band edge is reached.

We have thus shown how to control the symmetry character of the tunneling electrons: by filtering away the Δ_1 states, the Cr spacer acts as an analyzer of the secondary electronic symmetries that, in addition to Δ_1 at the $\bar{\Gamma}$ point, may contribute to tunneling transport across a simple MgO barrier. As an additional confirmation that, despite its ultrathin thickness x, the Cr layer acts as a tunnel barrier for Δ_1 electrons, we have inserted an additional Fe spacer between Cr and MgO at the lower junction interface. Taking into account the band structures of Fe and Cr [see Fig. 1(a)], this additional Fe spacer should confine Δ_1 electrons as discrete states in a QW [see Fig. 1(e)]. In our measurement geometry, a negative bias V injects electrons at E_F from the upper Fe electrode into the QW at an energy $E_F + eV$ [see Fig. 1(f)], while the well is probed only at E_F for all $V > 0$ [see Fig. 1(g)]. We therefore anticipate to observe QW states for $V < 0$ but not $V > 0$ *if* the ultrathin Cr indeed acts as a tunnel barrier for Δ_1 electrons, as observed for a *thick* Cr buffer layer [16]. Upon inserting an Fe spacer with thickness $7 < d < 21$ ML be-

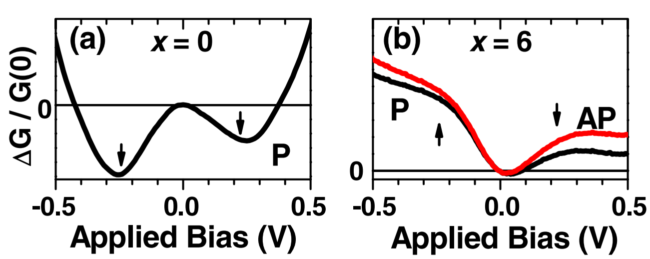

FIG. 4 (color online). Bias dependencies for Fe/Cr(x ML)/MgO/Fe MTJs of (a) $\Delta G_P(V)/G_P(0)$ for $x = 0$ and (b) $\Delta G_P(V)/G_P(0)$ and $\Delta G_{AP}(V)/G_{AP}(0)$ for $x = 6$.

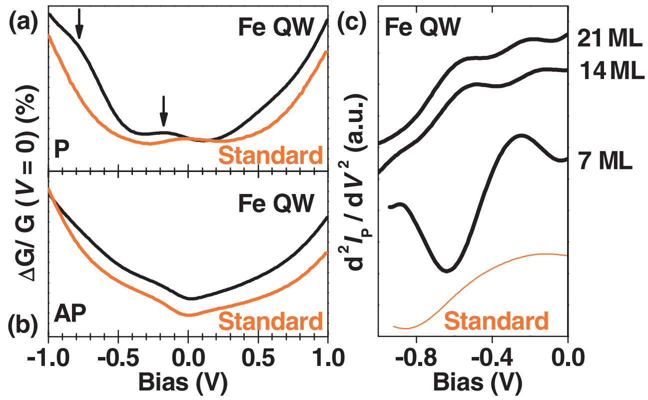

FIG. 5 (color online). Relative variation of $G_{P(AP)}(V)$ in standard Fe/MgO/Fe and Fe (7 ML) QW MTJs in the (a) P and (b) AP junction states. (c) $d^2I_P/dV^2(V)$ data for Fe/MgO/Fe and Fe(d) QW MTJs.

tween a uniform $x = 6$ ML Cr spacer and the MgO barrier, we experimentally observe that the TMR amplitude is restored to that of standard Fe/MgO/Fe junctions. We present in Fig. 5 measurements on MTJs that were patterned from a sample with a uniform $x = 6$ ML Cr spacer and an additional Fe spacer wedge with thickness $7 < d < 21$ ML below the 3 nm MgO barrier and the top Fe layer (hereafter called Fe QW MTJ). As seen in Fig. 5(a) for an Fe QW thickness of 7 ML, the aforementioned signature in $G_P(V)$ of a Δ_1 domination of conduction is again present, which underscores the TMR amplitude restoration. Furthermore, we observe shoulders in the G_P data at negative bias [see Fig. 5(a)]. This is enhanced in the bias dependence of $dG/dV = d^2I/dV^2$ [see Fig. 5(c)], which exhibits oscillations due to the formation of QW states at energies above E_F for given Fe QW thicknesses in qualitative agreement with theory [30]. No oscillations appear at positive bias as expected. No oscillations appear at negative bias in the AP junction state since, as discussed previously, G_{AP} is not dominated by Δ_1 states but rather by Δ_5 states that are not confined in the Fe QW. This experimental behavior confirms how ultrathin bcc Cr(001) indeed acts as a tunnel barrier for, and thus can filter, Δ_1 electrons.

To conclude, we have presented symmetry-conserved tunneling results that demonstrate how a metallic layer such as Cr can act as a tunnel barrier in a Fe/MgO(001) system. Such studies with appropriate spacer layers open valuable opportunities for future research on the nondominant electronic symmetries that, alongside defect states and interface states, can hamper large magnetoelectronic effects such as TMR, with immediate applications toward reducing the leakage current in epitaxial transistors. Such spacer layers can help distinguish between an intrinsic and an extrinsic (i.e., defect-mediated) origin to interlayer exchange coupling across epitaxial insulators [31,32], so as to consolidate this sister effect to GMR into a comprehensive foundation of magnetoelectronics across spacer layers.

The authors acknowledge D. Lacour for help with transport measurements. O. B. acknowledges ANR Grant No. 06-NANO-053-01 and CINES for supercomputer time (gem1100).

[1] M. N. Baibich *et al.*, Phys. Rev. Lett. **61**, 2472 (1988).
[2] J. E. Ortega *et al.*, Phys. Rev. B **47**, 1540 (1993).
[3] J. S. Moodera *et al.*, Phys. Rev. Lett. **74**, 3273 (1995).
[4] M. Bowen *et al.*, Appl. Phys. Lett. **79**, 1655 (2001).
[5] J. Faure-Vincent *et al.*, Appl. Phys. Lett. **82**, 4507 (2003).
[6] S. Yuasa *et al.*, Nat. Mater. **3**, 868 (2004).
[7] S. Parkin *et al.*, Nat. Mater. **3**, 862 (2004).
[8] C. Tiusan *et al.*, Phys. Rev. Lett. **93**, 106602 (2004).
[9] W. H. Butler *et al.*, Phys. Rev. B **63**, 054416 (2001).
[10] J. Mathon and A. Umerski, Phys. Rev. B **63**, 220403(R) (2001).
[11] Y. M. Lee *et al.*, Appl. Phys. Lett. **90**, 212507 (2007).
[12] X.-G. Zhang and W. H. Butler, Phys. Rev. B **70**, 172407 (2004).
[13] D. D. Djayaprawiraa *et al.*, Appl. Phys. Lett. **86**, 092502 (2005).
[14] S. Yuasa *et al.*, Appl. Phys. Lett. **89**, 042505 (2006).
[15] T. Zhu *et al.*, Phys. Rev. B **66**, 094423 (2002).
[16] T. Nagahama *et al.*, Appl. Phys. Lett. **79**, 4381 (2001).
[17] J. S. Moodera *et al.*, Phys. Rev. Lett. **83**, 3029 (1999).
[18] P. LeClair *et al.*, Phys. Rev. Lett. **86**, 1066 (2001).
[19] T. Nagahama *et al.*, Phys. Rev. Lett. **95**, 086602 (2005).
[20] P. LeClair *et al.*, Phys. Rev. B **64**, 100406(R) (2001).
[21] S. Yuasa, T. Nagahama, and Y. Suzuki, Science **297**, 234 (2002).
[22] M. Bowen *et al.*, Phys. Rev. B **73**, 140408(R) (2006).
[23] M. Bowen *et al.*, J. Phys. Condens. Matter **19**, 315208 (2007).
[24] C. Tiusan *et al.*, J. Phys. Condens. Matter **18**, 941 (2006).
[25] I. Turek *et al.*, *Electronic Structure of Disordered Alloys, Surfaces and Interfaces* (Kluwer, Dordrecht, 1997).
[26] J. Kudrnovský *et al.*, Phys. Rev. B **62**, 15 084 (2000).
[27] O. Bengone *et al.*, Phys. Rev. B **69**, 092406 (2004).
[28] K. D. Belashchenko, J. Velev, and E. Y. Tsymbal, Phys. Rev. B **72**, 140404(R) (2005).
[29] M. Bowen *et al.*, Phys. Rev. Lett. **95**, 137203 (2005).
[30] Z.-Y. Lu, X.-G. Zhang, and S. T. Pantelides, Phys. Rev. Lett. **94**, 207210 (2005).
[31] J. Faure-Vincent *et al.*, Phys. Rev. Lett. **89**, 107206 (2002).
[32] T. Katayama *et al.*, Appl. Phys. Lett. **89**, 112503 (2006).